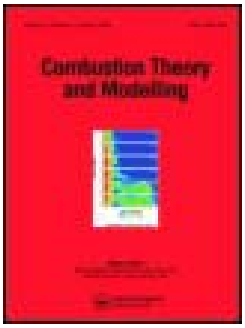

Combustion Theory and Modelling

ISSN: (Print) (Online) Journal homepage: https://www.tandfonline.com/loi/tctm20

Diffusion-controlled premixed flames

William A. Sirignano

To cite this article: William A. Sirignano (2020): Diffusion-controlled premixed flames, Combustion Theory and Modelling, DOI: 10.1080/13647830.2020.1863474

To link to this article: https://doi.org/10.1080/13647830.2020.1863474

Combustion Theory and Modelling, 2020
https://doi.org/10.1080/13647830.2020.1863474

Diffusion-controlled premixed flames

William A. Sirignano*

Department of Mechanical and Aerospace Engineering, University of California, Irvine, CA, USA

(*Received 27 July 2020; accepted 8 December 2020*)

Steady laminar flow structures with mixing, chemical reaction, and normal strain qualitatively representative of turbulent combustion at the small scales are analysed. A contrived counterflow configuration is examined to focus more easily on the premixed flames that are known to occur in multiple-flame structures; the premixed flame can be driven by a controlled heat source which is a surrogate for the diffusion flame in the practical multi-flame structure. Reduction to a one-dimensional similar form is obtained with density and properties variations. It is shown that premixed flames at fuel-rich or fuel-lean conditions sufficiently far from the stoichiometric condition are diffusion-controlled with a propagation velocity very weakly dependent on chemical kinetic details. In particular, heat diffused from a downstream source (i.e. the surrogate for a diffusion flame) is needed to sustain the flame. Effects of normal-strain rate, pressure level, and transport properties, combustible mixture composition, and heat source strength are determined through a parameter study with variations in Damköhler number, Prandtl number, upstream mass fractions of oxygen and propane fuel, and wall temperature. The premixed flame becomes less dependent on the downstream source as strain rate decreases and pressure increases. Small changes in heat and mass diffusivities have stronger effects than an order-of-magnitude change in Damköhler number.

Keywords: flamelet theory; premixed flames; diffusion control; multibranched flames; strained flames

1. Introduction

It is a honour to be invited to join the celebration for Professor Moshe Matalon who has made many outstanding contributions to combustion theory. His contributions to flame theory are among his most noteworthy, e.g. flame stretch, jump conditions, asymptotics, vorticity production, and multiple-flame structures [1–3] which inspired this author to select here a paper on flamelets.

There is need to understand the laminar mixing and combustion that occurs within turbulent eddies. These laminar flamelet sub-domains experience a significant strain rate. Some important work has been done here typically for counerflows or simple vortex structures in two-dimensions or axisymmetry and often with a constant-density approximation [4–10]. Linan [4] and Peters [9] studied the counterflow configuration. Karagozian and Marble [6] examined a three-dimensional flow with radial inward velocity, axial jetting, and a vortex centred on the axis. Pierce and Moin [10] fixed domain size and reduced the advection by forcing flux to zero at the boundaries.

These models are built around the assumption that the flamelets are always nonpremixed (i.e. diffusion) flames and subject to flow strain rate. The Pierce-Moin flamelet approach

*Email: sirignan@uci.edu

was employed [11,12] in the simulation of a single-injector rocket engine, showing the importance of flamelets undergoing high strain rates. Contradictions occurred since both premixed flames and nonpremixed flames appeared in the predictions, largely through multi-branched flames; in particular, the combination is often seen of a fuel-lean premixed-flame branch with a branch consisting of a merged diffusion flame and fuel-rich premixed flame.

Experiments and asymptotic analysis [13] indicate that a partially premixed fuel-lean flame and a diffusion flame are able to co-exist in a counterflow with opposing streams of heptane vapour and methane-oxygen-nitrogen mixture. An improved flamelet theory is required to address both premixed and non-premixed flames. Sirignano [14,15] developed a counterflow analysis with three-dimensional strain showing the possibility for a variety of flame configurations to exist depending on the compositions of the inflowing streams: (i) three flames including fuel-lean partially premixed, nonpremixed (i.e. diffusion-controlled), and fuel-rich partially premixed; (ii) nonpremixed and fuel-rich partially premixed; (iii) fuel-lean partially premixed and nonpremixed; (iv) nonpremixed; and (v) premixed. López et al. [16,17] have extended the counterflow analysis to consider detailed kinetics for methane-oxygen detailed chemical kinetics. Multi-branched flames in a mixing layer with imposed counterflow has recently been studied [18]. There, both shear strain rates and normal strain rates are important.

Results with multi-flame structures [15–18] indicate that the highest temperature in the counterflow exists at the diffusion flame. If the inflowing combustible mixture is sufficiently far from stoichiometric proportion of fuel and oxygen, the premixed flame stands within the diffusion layer of the diffusion flame and receives heat that conducts against the incoming stream. The advection velocity at the premixed flame does not vary strongly with modifications in the chemical kinetic rate. It can remain within the diffusion layer over a wide parameter range. Thereby, the propagation of the premixed flame does not follow the behaviour of the classical isolated premixed flame. It appears that the heat supplied to the premixed flame by the diffusion flame is an important factor in the sustenance of the premixed flame at these very lean and very rich mixture ratios.

This behaviour for counterflow flames is also known to exist for multibranched flames, e.g. triple flames [19,20]. The diffusion flame has the highest temperature. Jordà Juanós and Sirignano [19] have noted the pentasectional character of triple flames whereby each premixed flame has two sections. In the downstream section where the mixture is further from the stoichiometric condition and closer to the flammability limit, the flame shows clear signs of diffusion control. Recently, Rajamanickam [20] has provided an interesting three-dimensional triple-flame analysis where normal strain is applied to the triple flame structure through an imposed counterflow.

A goal in this paper is to gain a better understanding of how the premixed flame is sustained for an upstream mixture ratio that is far from the stoichiometric value. A study is made of a contrived configuration that eliminates details in the practical case that do not affect the essence of the premixed behaviour. A combustible mixture of oxygen, propane, and an inert gas flow against a hot wall yielding a stagnation-point flow that has a similarity with one side of a counterflow. The premixed flame exists in this inflow towards the wall. The hot wall acts as a surrogate for the diffusion flame found in multi-branched flame structures. It can provide heat to the premixed flame if that flame remains within the diffusion layer at the wall. It is known that radicals produced in the diffusion flame could diffuse to the premixed flame and help ignition. Within our one-step kinetics framework, that will not be directly modelled. Combustion with variable density will be examined

here. The velocity in the normal direction to the wall generally decreases as the wall is approached; however, the decrease is commonly not strictly monotonic because of density variations. Propane and oxygen are considered with one-step kinetics [21]; however, the qualitative conclusions are expected to be more general. Those one-step kinetic relations were obtained by fitting to experiments for premixed flames.

The analysis of the stagnation-point flow with the premixed flame is given in the next section. Results are given in Section 3 while concluding remarks are stated in Section 4.

2. Analysis

The guiding partial differential equations for a steady, two-dimensional, reacting stagnation-point flow are established in Sub-section 2.1 with the chemical-kinetic model detailed in Sub-section 2.2. The similar form yielding ordinary differential equations is developed in Sub-section 2.3. The numerical method for solution is described in Sub-section 2.4.

2.1. *Two-dimensional planar flow formulation*

Consider the x direction parallel to the hot wall with the normal to the wall in the y direction. u and v are respectively the x and y components of velocity. The wall lies at $y = 0$ and the incoming flow is in the positive y domain but the v component of velocity is negative. Standard low-Mach-number approximations are used. Fickian mass diffusion, Fourier heat conduction, and Newtonian viscosity are considered. Mass and thermal diffusivities are assumed to be identical. The Prandtl number (Pr) is constant but may take non-unitary values. The product of density ρ and dynamic viscosity μ is constant throughout the field. A perfect gas is assumed. The governing equations for steady, two-dimensional flow are given as

$$\frac{\partial(\rho u)}{\partial x} + \frac{\partial(\rho v)}{\partial y} = 0 \tag{1}$$

$$\rho u\frac{\partial u}{\partial x} + \rho v\frac{\partial u}{\partial y} = \frac{\partial}{\partial y}\left(\mu\frac{\partial u}{\partial y}\right) \tag{2}$$

$$\rho u\frac{\partial h}{\partial x} + \rho v\frac{\partial h}{\partial y} = \frac{1}{Pr}\frac{\partial}{\partial y}\left(\mu\frac{\partial h}{\partial y}\right) - \rho\Sigma_{m=1}^{N} h_{f,m}\omega_m \tag{3}$$

$$\rho u\frac{\partial Y_m}{\partial x} + \rho v\frac{\partial Y_m}{\partial y} = \frac{1}{Pr}\frac{\partial}{\partial y}\left(\mu\frac{\partial Y_m}{\partial y}\right) + \rho\omega_m\ ;\ m = 1, 2, \ldots, N \tag{4}$$

An exact solution of the variable-density Navier-Stokes equation can be obtained subject to determination of ρ and μ through solutions of the energy and species equations as discussed below. There is no need for use of a boundary-layer approximation. Thus, the solution here is the natural solution, subject to neglect of terms of $O(x^2)$. The variable density and viscosity case requires some couplings for Equations (1) and (2) with Equations (3) and (4) and with an equation of state and fluid-property laws which affect ρ and μ.

Here, the sensible enthalpy $h = c_p T$ is based on the assumption of a calorically perfect gas. When normalised by ambient conditions, the non-dimensional values of enthalpy and

temperature are identical. For simplification, we neglect the effect of species composition on specific heats and the specific gas constant.

In general, each of the species equations must be solved. However, for the special case assumed here of a one-step chemical reaction, each species is consumed or produced at a rate in direct proportion to the rate of some other species that is produced or consumed. Therefore, Equation (4) need only be solved for fuel mass fraction Y_F and oxygen mass fraction Y_O. For the one-step kinetics considered here, the last term in Equation (3) may be replaced by $-\rho Q\omega_F$ where Q is the heating value (energy/mass) of the fuel and $\omega_F < 0$ is the chemical oxidation rate of the fuel. $\nu = 0.275$ is the stoichiometric ratio of propane mass to oxygen mass.

From these primitive equations for h and Y_m, we may form equations for conserved scalars. We define two conserved scalars as

$$\begin{aligned} \alpha &\equiv Y_F - \nu Y_O \\ \beta &\equiv h + \nu Y_O Q \end{aligned} \tag{5}$$

to obtain

$$\begin{aligned} \rho u\frac{\partial \alpha}{\partial x} + \rho v\frac{\partial \alpha}{\partial y} &= \frac{1}{Pr}\frac{\partial}{\partial y}\left(\mu\frac{\partial \alpha}{\partial y}\right) \\ \rho u\frac{\partial \beta}{\partial x} + \rho v\frac{\partial \beta}{\partial y} &= \frac{1}{Pr}\frac{\partial}{\partial y}\left(\mu\frac{\partial \beta}{\partial y}\right) \end{aligned} \tag{6}$$

Note that, for the non-reacting case, h and Y_m are conserved scalars satisfying this same partial differential equation.

Equations (3) and (4) are $N + 1$ equations describing the solutions for enthalpy and all mass fractions. We need consider only $N - 1$ species equations plus the energy equation because the mass fractions are known to sum to the value of one. Considering only the two reactants, we obtain three equations for h, Y_F and Y_O. Equations (6) are not independent as implied by Equation (5); however, they avoid the reaction-rate term and its associated computational stiffness. Thus, we choose to use the three Equations (3) and (6) with the two relations from (5) to obtain to obtain h, Y_F, Y_O, α, and β.

The above equations can be considered as non-dimensional if we choose certain reference values for normalisation. The superscript * will be used to designate a dimensional property. S^* is the normal rate of strain in the incoming flow. That is, at $y = \infty$ where density is uniform, $S^* = \partial u^*/\partial x^* = -\partial v^*/\partial y^*$. The variables u^*, v^* are normalised by $[S^*\mu^*_\infty/\rho^*_\infty]^{1/2}$; t^* is normalised by $(S^*)^{-1}$ while x, y are normalised by $[\mu^*_\infty/(\rho^*_\infty S^*)]^{1/2}$. ρ^*, h^*, p^*, and ω^*_m are normalised respectively by $\rho^*_\infty, S^*\mu^*_\infty/\rho^*_\infty, S^*\mu^*_\infty$, and S^*. Properties $\mu^*, \lambda^*/c^*_p$, and D^* are normalised by μ^*_∞, μ^*_∞, and $\mu^*_\infty/\rho^*_\infty$, respectively. Note that the reference length $[\mu^*_\infty/(\rho^*_\infty S^*)]^{1/2}$ is the estimate for the magnitude of the viscous-layer thickness. In the remainder of this article, the non-dimensional forms of the above equations will be considered.

The stagnation point in the steady counterflow will be taken as the origin $x = y = 0$. Along the line $x = 0$ normal to the interface, we can expect the first derivatives of v, ρ, h, T, and Y_m with respect to x to be zero-valued. The velocity component u is an odd function of x, going through zero and changing sign at that line. Consequently, upon neglect of terms of $O(x^2)$ the variables v, ρ, h, T, and Y_m can be considered to be functions only of y.

The boundary conditions on Equations (2) through (4) involve specifications of the dependent variables at $y = \infty$ and $y = 0$. At the hot wall ($y = 0$), the mass fractions of

oxygen and propane go to zero value and the temperature is held at a constant value which is generally higher than the premixed flame temperature. This allows the wall to be considered as a surrogate diffusion flame. The normal velocity goes to zero at the wall and the tangential velocity is allowed to slip; i.e. there is no shear force there. At $y = \infty$, the mass fractions, temperature, conserved scalars, and rate of normal strain are specified constants. The constant normal strain rate implies that u is proportional to x while v is proportional to y in the incoming flow far upstream of the flame and diffusion layer.

It can be shown [14] that with neglect of terms of $O(x^2)$ the variables v, h, Y_m, α, and β will depend only on y. It follows that our equations give exact Navier-Stokes solutions without need for the boundary-layer approximation within the $O(x^2)$ error bound. Furthermore, a similar solution can be found which is one-dimensional in nature and is governed by a system of ordinary differential equations.

2.2. *Chemical rate model*

The equations in the prior sub-section apply for a premixed flame in a stagnation-point flow. We will focus on propane-oxygen flows with one-step chemical kinetics. Nevertheless, results will be qualitatively more general, applying to situations with more detailed kinetics and to other hydrocarbon/oxygen-or-air combination. See, for example, the detailed-kinetics studies for counterflow flames [16,17] in comparison with the one-step-kinetics study for counterflow flames [15]. Westbrook and Dryer [21] kinetics are used; they were developed for premixed flames. It results that

$$\omega_F^* = -A^* \rho^{*0.75} Y_F^{0.1} Y_O^{1.65} e^{-50.237/\tilde{h}} \tag{7}$$

The ambient temperature is set at 300 K and density ρ^* is given in units of kilograms per cubic metre. Here, $A^* = 4.79\text{x}10^8 (kg/m^3)^{-0.75}/s$ with the dimensional strain rate S^* used to normalise time and reaction rate. In non-dimensional terms,

$$\begin{aligned} \omega_F &= -\frac{A^* {\rho_\infty^*}^{0.75}}{S^*} \tilde{h}^{-0.75} Y_F^{0.1} Y_O^{1.65} e^{-50.237/\tilde{h}} \\ \omega_F &= -\frac{Da}{\tilde{h}^{0.75}} Y_F^{0.1} Y_O^{1.65} e^{-50.237/\tilde{h}} \end{aligned} \tag{8}$$

This relation defines the Damköhler number Da. There is no need to set pressure (or its proxy, density) and the strain rate separately for a one-step reaction. For convenience, $Da \equiv KDa_{ref}$ where

$$Da_{ref} \equiv \frac{\tilde{A}(10\,\text{kg/m}^3)^{0.75}}{(10/\text{s})} = 2.693\ x\ 10^7; \quad \text{K} \equiv \left[\frac{\rho_\infty^*}{10\,\text{kg/m}^3}\right]^{0.75} \frac{10/\text{s}}{S^*} \tag{9}$$

$10\,\text{kg/m}^3$ and $10/\text{s}$ are arbitrarily chosen as reference values for density and strain rate, respectively. The reference value for density implies an elevated pressure. The strain-rate reference value is in the middle of an interesting range for this chemical reaction. For propane and oxygen, the mass stoichiometric ratio $\nu = 0.275$.

K will increase (decrease) as the strain rate decreases (increases) and/ or the pressure increases (decreases). $K = 1$ is our base case and the range covered will vary by an order of magnitude.

2.3. *Similar form*

We follow now standard stagnation-flow analysis [22]. The density-weighted Illingworth transformation of y can be used to replace y with $\eta \equiv \int_0^y \rho(y')\,\mathrm{d}y'$. The scalar variables and the v component of velocity are taken as functions of y (or η) alone. Neglect of terms of $O(x^2)$ implies that the velocity component u is proportional to the product of x and a function of η. Specifically, we define $f(\eta)$ and thereby $df/d\eta$ so that $u = Sx(df/d\eta)$. At the edge of the viscous layer at large positive η, $df/d\eta \to 1$ and $f \to \eta$. The integration of the continuity equation yields

$$\rho v = -f(\eta) \tag{10}$$

The independence of pressure p and $\partial p/\partial y$ on x implies that $\partial^2 p/\partial y \partial x = 0$ which is useful in constructing a third-order ordinary differential equation for $f(\eta)$ [15]. Then, second-order ordinary differential equations can be created for the scalar variables. We define $\tilde{h}(\eta) \equiv h^*(\eta)/h^*(\infty) = h(\eta)/h_\infty$. The resulting system of ordinary differential equations and boundary values follows with the prime used to indicate ordinary differentiation with respect to η. For example, $f' \equiv df/d\eta$ and $f'' \equiv d^2 f/d\eta^2$.

$$\begin{aligned} f''' + ff'' &= (f')^2 - \tilde{h} \\ f(0) = 0\ ;\ f''(0) &= 0\ ;\ f'(\infty) = 1 \\ \tilde{h}'' + Prf\tilde{h}' &= Pr\tilde{Q}\omega_F \\ \tilde{h}(0) = \frac{h(0)}{h_\infty}\ ;\ \tilde{h}(\infty) &= 1 \end{aligned} \tag{11}$$

$$\begin{aligned} Y_F'' + PrfY_F' &= Pr\omega_F \\ Y_F(0) = 0\ ;\ Y_F(\infty) &= Y_{F,\infty} \\ Y_O'' + PrfY_O' &= Pr\omega_F/\nu \\ Y_O(0) = 0\ ;\ Y_O(\infty) &= Y_{O,\infty} \end{aligned} \tag{12}$$

where $\tilde{Q}$ is the fuel heating value normalised by the enthalpy at plus infinity. For a perfect gas with constant specific heat, the nondimensional enthalpy $\tilde{h}$ also equals the temperature normalised by the temperature at plus infinity.

There is an option to reduce the number of stiff differential equations by replacing two of the three equations for the reactive scalars $\tilde{h}$, Y_F, and Y_O by the two equations for conserved scalars. Those two differential equations with their boundary values are

$$\begin{aligned} \alpha'' + Prf\alpha' &= 0 \\ \alpha(0) = 0\ ;\ \alpha(\infty) &= \alpha_\infty = Y_{F,\infty} - \nu Y_{O,\infty} \\ \beta'' + Prf\beta' &= 0 \\ \beta(0) = \tilde{h}(0)\ ;\ \beta(\infty) &= \beta_\infty = 1 + \nu Y_{O,\infty}\tilde{Q} \end{aligned} \tag{13}$$

In the study of the strength of the premixed flame, it is useful to examine the integral of the reaction rate over the field. In particular, we calculate $I_\omega \equiv \int_0^\infty \omega_F\,\mathrm{d}\eta = \int_0^\infty \omega_F \rho\,\mathrm{d}y$. This essentially is an integral of reaction rate per unit-volume over the total volume since ω_F will not vary in the transverse direction and depends only on y.

2.4. *Numerical method*

The system of ordinary differential equations with boundary values is solved numerically using a relaxation method and central differences. Specifically, we solve Equations (11) and (13) for f, h, α, and β, using Equation (5) to obtain Y_F and Y_O. Solution over the range $0 \leq \eta \leq 8$ with 720 uniformly-spaced mesh points provides adequate fittings to the asymptotic behaviours as $y \to \infty$. The parameters that are varied are $K, Pr, Y_{F,\infty}, Y_{O,\infty}$ and $\tilde{h}(0)$. Most calculations have $Pr = 1, K = 1$, and $\tilde{h}(0) = 8$ with emphasis on the effect of upstream mixture ratio, i.e. $Y_{F,\infty}$ and $Y_{O,\infty}$. Fuel-lean, stoichiometric, and fuel-rich conditions are addressed. However, the effects of Pr, K, and $\tilde{h}(0)$ variations are shown as well.

3. Results

Results have been obtained for the scalar properties, reaction rates, and velocity components. Fuel-to-oxidiser mixture mass ratios vary from 0.0688 to 3.33 where the stoichiometric value is 0.275. The Damköhler coefficient K varies from 0.3 to 3 while Prandtl number Pr varies from 0.7 to 1.3. The normalised wall temperature $h(0)/h_\infty$ varies from 3.0 to 8.0. If not otherwise specified in a figure caption, the base values apply: $Pr = 1.0$, $K = 1.0$, and $h(0)/h_\infty = 8.0$. Plots of dependent variables versus the density-weighted variable η are presented. Thus, for a given value of η, the y-distance from the wall increases as the temperature in the diffusion layer increases and/or the pressure decreases. Specifically,

$$y = \int_0^\eta \frac{1}{\rho}\, \mathrm{d}\eta' \tag{14}$$

As a remedy for the classical cold-boundary challenge for premixed-flame analysis, $\omega_F = 0$ for $\tilde{h} = h/h_\infty = T/T_\infty < 2$ was imposed. No meaningful difference occurred in tests where the bound was $T/T_\infty < 3$.

The configuration has inflow from large positive values of y for all x values, outflow at large positive and negative values of x for all y values, and no flow through the $y = 0$ plane. Thereby, for fixed strain rate and ambient density, the mass flux per unit area through any y plane decreases as y decreases. The flame structure depends only on y and is independent of x. Mass burning rate per unit area consequently must decrease as the y value for the flame position decreases. For prescribed incoming composition, ambient density, ambient strain rate, wall temperature, transport properties and pressure, the premixed flame will stabilise at a y position where the mass burning rate equals the mass flux in the negative-y direction locally.

In the next subsection, the effect of mixture ratio on the flame behaviour is examined. In the other subsections, the effects of wall temperature, pressure and normal compressive strain (through the Damköhler number), and Prandtl number are determined.

3.1. *Effect of mixture ratio*

Upstream mixture ratios will be varied first with other parameters held constant. In Figures 1 and 2, results for the stoichiometric case and several fuel-lean cases are compared. In four cases, mass mixture ratio varies from 0.275 down to .0688. In the stoichiometric case and the least-lean case (mixture ratio of 0.2064), the premixed flame is seen to stabilise outside of the wall diffusion layer. That is, heat conduction from the hot

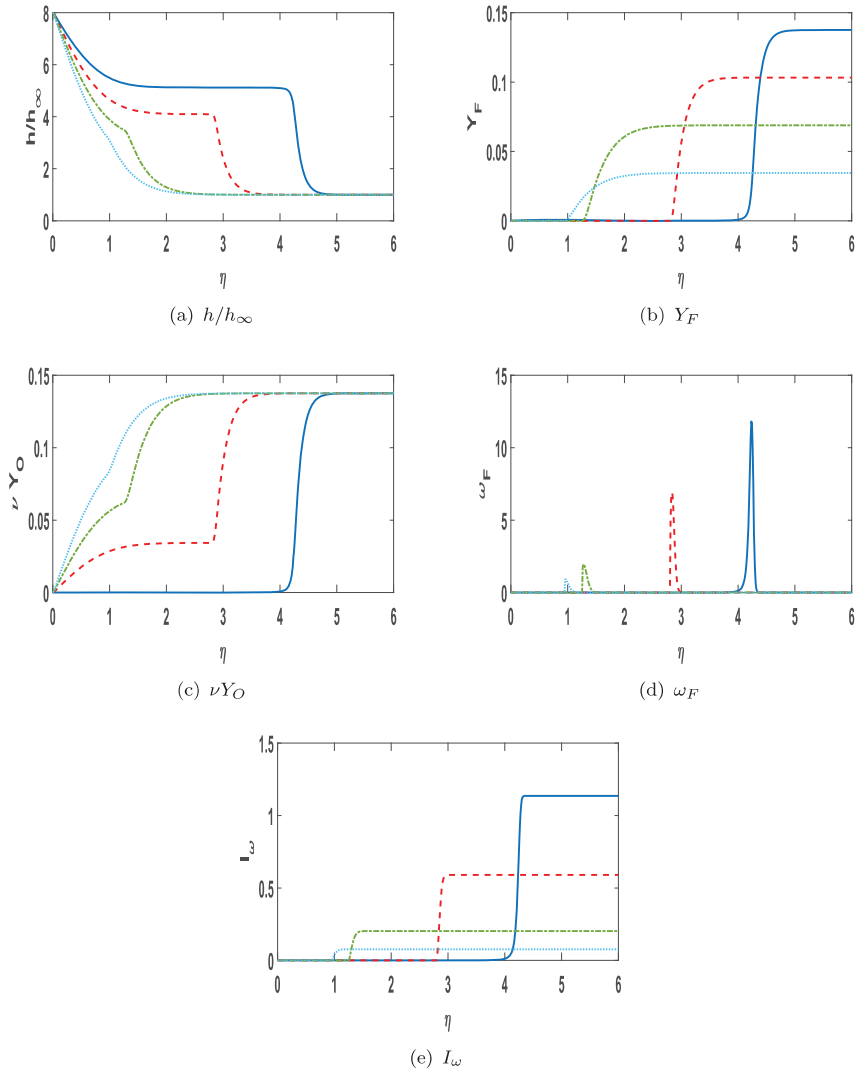

Figure 1. Lean premixed flame at various mixture ratios: scalar properties. $Y_{O,\infty} = 0.5, Y_{F,\infty} = 0.1375$ (stoichiometric) blue solid, 0.1032 red dashed, 0.0688 green dot-dash, 0.0344 light blue dot. (a) h/h_∞. (b) Y_F. (c) νY_O. (d) ω_F. (e) I_ω.

wall does not affect the flame as shown in Figure 1(a) while 1(b) indicates that the fuel is consumed before it advects into the wall diffusion layer. The behaviours of the oxygen mass fraction in 1(c) and the reaction rate in 1(d) are consistent with this understanding.

As expected, Figure 1(e) shows that the integrated reaction rate increases as the stoichiometric condition is approached. This result is consistent with the finding in Figure 2(a) that the mass flux and thereby the mass burning rate) increases as stoichiometry is approached with constant boundary temperatures, pressure, and imposed normal strain rate.

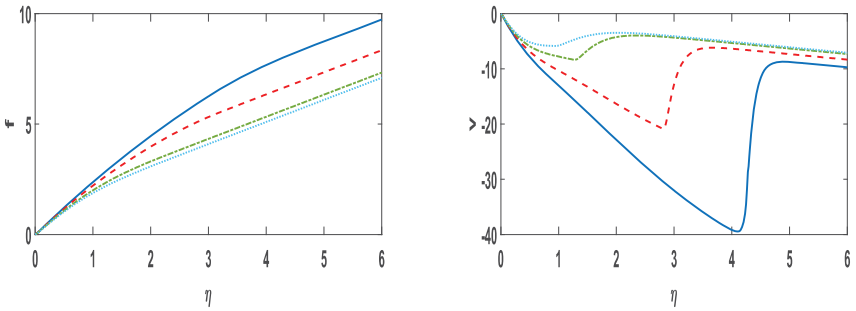

(a) f (b) v

(c) $u/(Sx)$

Figure 2. Lean premixed flame at various mixture ratios: mass flux and velocity field. $Y_{O,\infty} = 0.5$, $Y_{F,\infty} = 0.1375$ (stoichiometric) blue solid, 0.1032 red dashed, 0.0688 green dot-dash, 0.0344 light blue dots. (a) f. (b) v. (c) $u/(Sx)$.

Now, examination of the two very lean cases (mixture ratios of 0.1375 and 0.0688) indicates a very different behaviour. The flames stand within the wall heat-diffusion layer, i.e. $\eta < 2$. They receive a substantial amount of conducted heat from the wall. As expected, burning rates are lower, decreasing as the mixture becomes more lean. Even though the integrated reaction rate in Figure 1(e) shows a variation in magnitude by a factor greater than 2, the flame speed indicated in 2(b) varies only slightly. Here, clear signs of diffusion control rather than classical premixed flame behaviour are found. These very lean flames need a host to provide heat. Later, it will be shown that these flames will not exist without the heat source.

Figure 2(c) shows that the transverse velocity will increase as the wall is approached because of the expansion due to heating from both the wall and the exothermic reaction. If the no-slip condition were applied at the wall, the u component of velocity would first increase as the wall is approached, then decrease within the viscous layer [14]. Comparison of the three sub-figures shows that u, $|v|$, and f all increase as the mixture moves towards stoichiometric conditions and becomes more energetic in terms of energy released per unit time per unit volume. it is obvious that u and $|v|$ would show similar increase if plotted versus y.

Four fuel-rich cases are studied with results presented in Figures 3 and 4; the mixture ratios are 1.0, 2.0, 5.0, and 6.67. The least-rich case is the only one showing the classical premixed-flame character without dependence on a host to provide heat. The other three

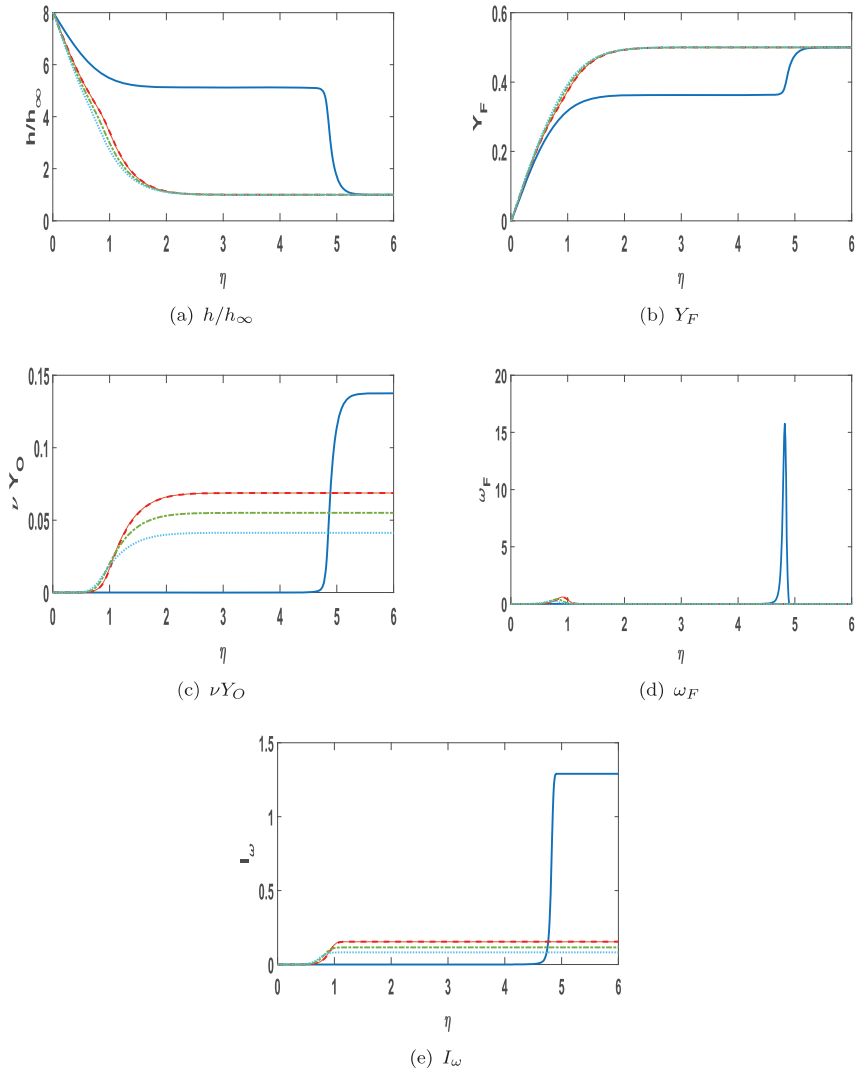

(a) h/h_∞ (b) Y_F (c) νY_O (d) ω_F (e) I_ω

Figure 3. Rich premixed flame at various mixture ratios: scalar properties. $Y_{F,\infty} = 0.5$, $Y_{O,\infty} = 0.500$ blue solid, 0.250 red dashed, 0.200 green dot-dash, 0.150 light blue dots. (a) h/h_∞. (b) Y_F. (c) νY_O. (d) ω_F. (e) I_ω.

cases have the flame standing in the wall diffusion layer with the flame speed and location showing very little sensitivity to the mixture ratio value. The same qualitative trends occur in both fuel-lean and fuel-rich cases as the mixture changes in the direction of stoichiometric conditions. Again, diffusion control is evident for mixtures far from stoichiometric proportions.

It is noteworthy that although a compressive normal strain is imposed on the incoming flow in the negative y-direction, the heat release with gas expansion causes a local zone of tensile normal strain in both the y and x directions, as shown by the variation of slope

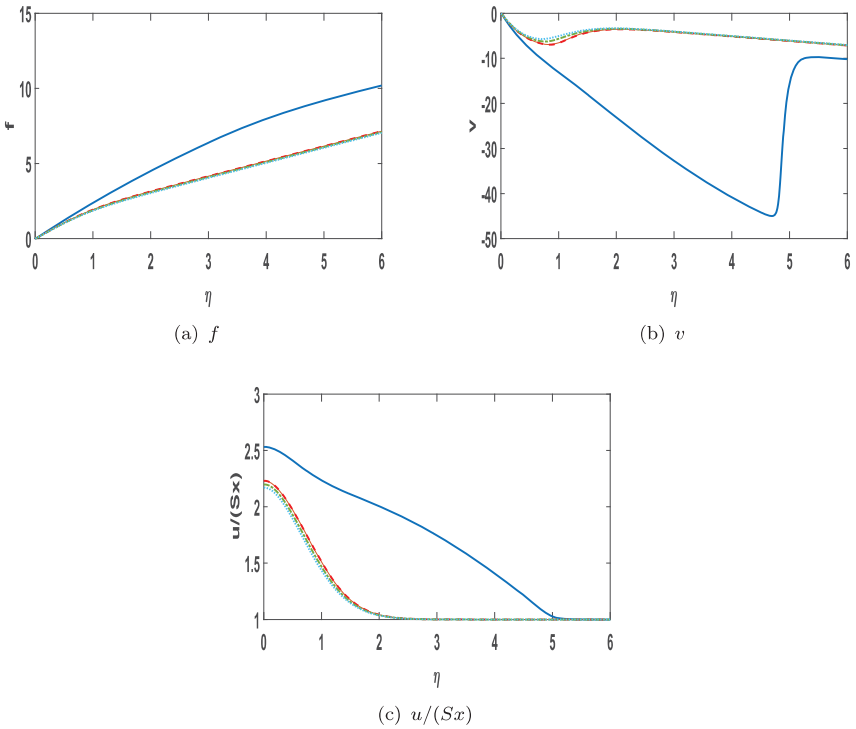

(a) f (b) v

(c) $u/(Sx)$

Figure 4. Rich premixed flame at various mixture ratios: mass flux and velocity field. $Y_{F,\infty} = 0.5$, $Y_{O,\infty} = 0.500$ blue solid, 0.250 red dashed, 0.200 green dot-dash, 0.150 light blue dots. (a) f. (b) v. (c) $u/(Sx)$.

in Figures 2(b) and 4(b). This has been noted before [14,15,18] but generally has been ignored elsewhere in discussion of the strain in flamelets.

A comparison of the relation between flame speed and reaction rate is made for seven of the cases shown in Figures 1 through 4. Three cases are fuel lean, one is stoichiometric, and three cases are fuel-rich. Results are shown in Table 1 with fuel/air mass mixture ratio increasing as the table is descended. The forward position of the premixed flame front is denoted by η^*. The figures for h/h_∞, Y_F, and Y_O indicate that the diffusion layer extends almost to $\eta = 3$. Thus, the flames for the stoichiometric case and the two cases with nearest

Table 1. Relation between flame speed and reaction rate as function of mixture ratio.

Mixture Ratio	$Y_{O,\infty}$	$Y_{F,\infty}$	Flame Location	v_{flame}	$I_{\omega,\infty}$	$\frac{\lvert v_{flame}\rvert}{\sqrt{I_{\omega,\infty}}}$
0.0688	0.500	0.0344	$\eta^* = 2.05$	−3.476	0.0769	12.535
0.1375	0.500	0.0688	$\eta^* = 2.36$	−3.969	0.2025	8.820
0.2064	0.500	0.1032	$\eta^* = 3.68$	−6.176	0.5902	8.040
0.2750	0.500	0.1375	$\eta^* = 4.90$	−8.741	1.136	8.202
1.000	0.500	0.500	$\eta^* = 5.47$	−9.783	1.295	8.596
2.000	0.250	0.500	$\eta^* = 2.08$	−3.554	0.1548	9.033
3.333	0.150	0.500	$\eta^* = 1.95$	−3.341	0.0817	11.696

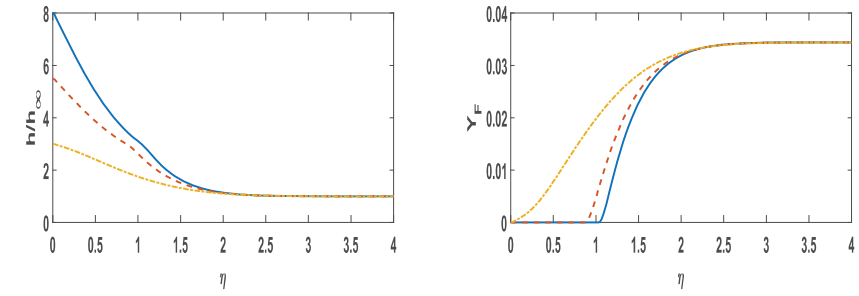

(a) h/h_∞

(b) Y_F

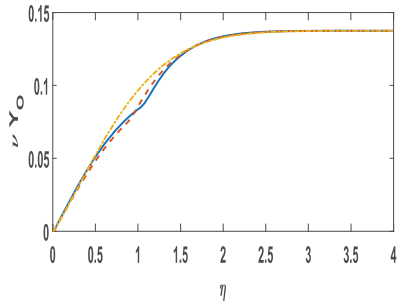

(c) νY_O

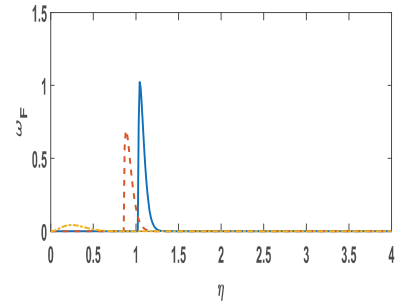

(d) ω_F

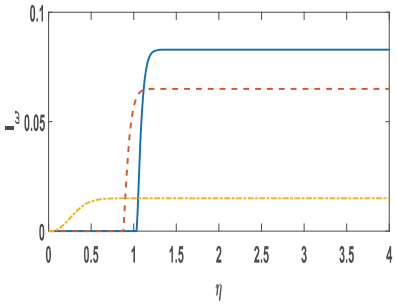

(e) I_ω

Figure 5. Lean premixed flame at various wall temperatures: scalar properties. $K = 3.0$, $Y_{F,\infty} = 0.0344$, $Y_{O,\infty} = 0.500$, $h(0)/h_\infty = 8.0$ blue solid, 5.5 red dashed, 3.0 orange dot-dash. (a) h/h_∞. (b) Y_F. (c) νY_O. (d) ω_F. (e) I_ω.

mixture ratio in the order (ie., one lean and one rich) lie outside the thermal layer. Classical premixed flame theory informs us that the flame speed should increase with the square root of the averaged reaction rate. We assume that our integrated global reaction rate I_ω and the average are proportioned. We identify the flame speed by the absolute value of v at its local minimum point in Figures 2(b) and 4(b) before the magnitude of v increases with the negative-y flow direction due to expansion from heat release.

The values of $|v_{flame}|/\sqrt{I_\omega}$ for the flames outside of the thermal layer match within a few per cent. Deviations of that measure grow for the other fuel-lean and fuel-rich cases

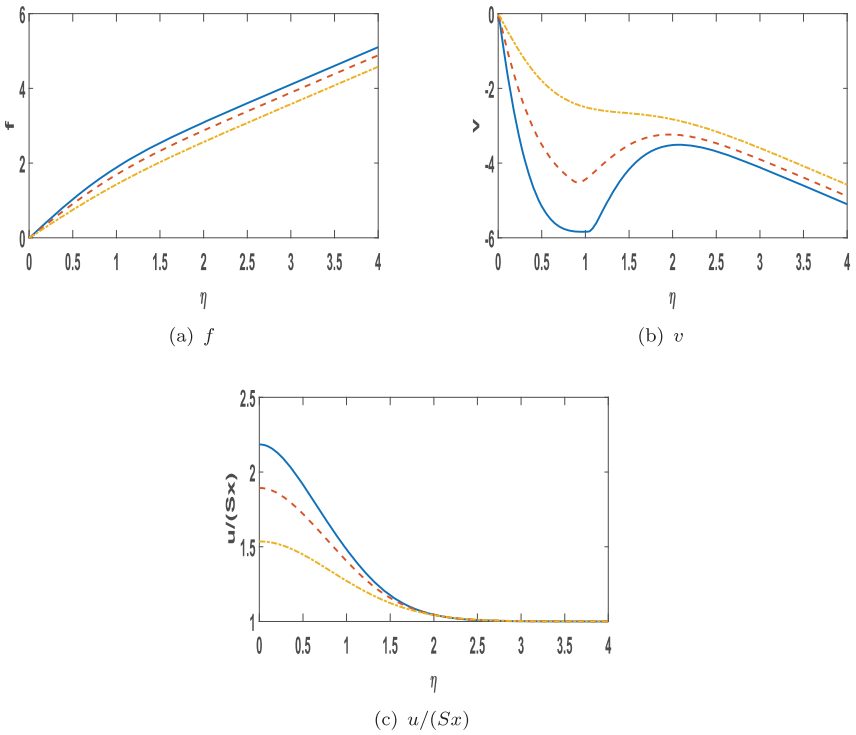

(a) f (b) v

(c) $u/(Sx)$

Figure 6. Lean premixed flame at various wall temperatures: mass flux and velocity field. $K = 3.0$, $Y_{F,\infty} = 0.0344$, $Y_{O,\infty} = 0.500$, $h(0)/h_\infty = 8.0$ blue solid, 5.5 red dashed, 3.0 orange dot-dash. (a) f. (b) v. (c) $u/(Sx)$.

where the flame stands within the thermal layer. So, those flames within the diffusion layer are experiencing a different mechanism to determine the propagation speed. The available evidence indicates that it is driven thermally by heating from the wall. As the mixture ratio moves away from the near-stoichiometric domain, in either the fuel-rich or fuel-lean direction, the reaction rate decreases and the flame speed decreases as expected. Note, however, that when the flame sits in the thermal layer with heat addition from the wall, the factor $|v_{flame}|/\sqrt{I_\omega}$ increases substantially, indicating the flame speed is greater than what would result from self-generated heat alone.

The results here are consistent with the findings of Jordà Juanós and Sirignano [19]. Namely, as the mixture ratio gets further from the stoichiometric value, the premixed flame deviates substantially from the classical premixed flame in both its qualitative and quantitative characteristics. For example, flame propagation for the classical flame depends strongly on both diffusion and reaction whereas, for these weaker flames, diffusion influence is stronger.

3.2. *Effect of heat source*

Next, the effect of wall temperature on a very lean case (ratio of 0.0688) is determined. The Da is increased with $K = 3.0$. Figures 5 and 6 show the increased Da does not make the flame independent of wall heating. As the wall temperature decreases from $\tilde{h}(0) = 8$

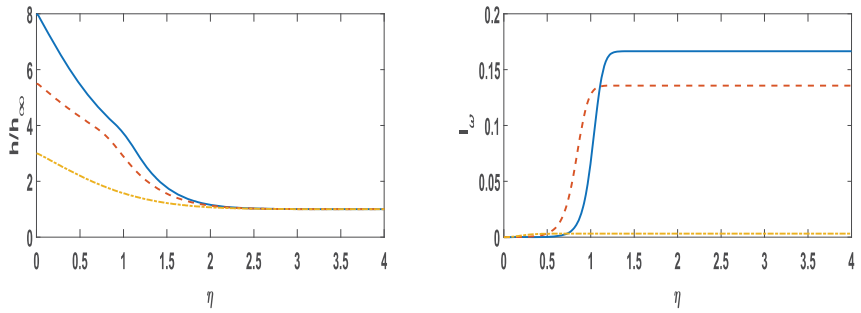

(a) h/h_∞ (b) I_ω

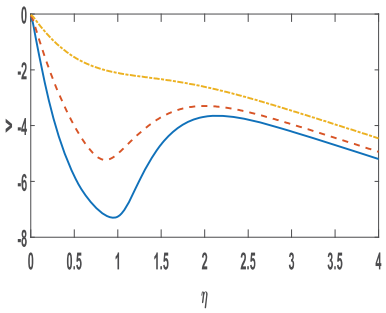

(c) v

Figure 7. Rich premixed flame at various wall temperatures: mass flux and velocity field. $K = 3.0$, $Y_{F,\infty} = 0.500$, $Y_{O,\infty} = 0.250$, $h(0)/h_\infty = 8.0$ blue solid, 5.5 red dashed, 3.0 orange dot-dash. (a) h/h_∞. (b) I_ω. (c) v.

to values of 5.5 and then 3.0, the flame weakens and moves closer to the heat source. The mass burning rate decreases. In fact, in our abstract situation, for the lowest wall temperature, some of the fuel 'diffuses into the wall' without burning. This is caused by the wall boundary condition which was conveniently chosen to have the wall be a surrogate for a diffusion flame. With reduced assistance from wall heating (due to reduced wall temperature), the burning-rate must be reduced and flame speed must decrease causing the flame to stabilise closer to the wall where the v velocity is lower. Again, the collective evidence shows the behaviour as diffusion-controlled for the very lean mixture.Figure 7 shows the same qualitative behaviours for the fuel-rich case (with mass mixture ratio of 2.00) that are seen in the fuel-lean case. The general observation is that the trend as wall temperature decreases for a given incoming mixture is the same as the trend for variation of mixture away from stoichiometry at fixed wall temperature. Clearly, the mixture further from stoichiometric conditions is more dependent on heat supplied by the wall.

3.3. *Effect of Damköhler number*

The effect of normal strain rate and pressure are displayed through variation of Da in Figure 8 for a very lean mixture ratio of 0.0688 and in 9 for a very rich mixture ratio of 2.0. Da is varied by an order of magnitude with the values $K = 0.3, 1.0$, and 3.0. An increase in Da does strengthen the flame for either mixture but only slightly. We do not

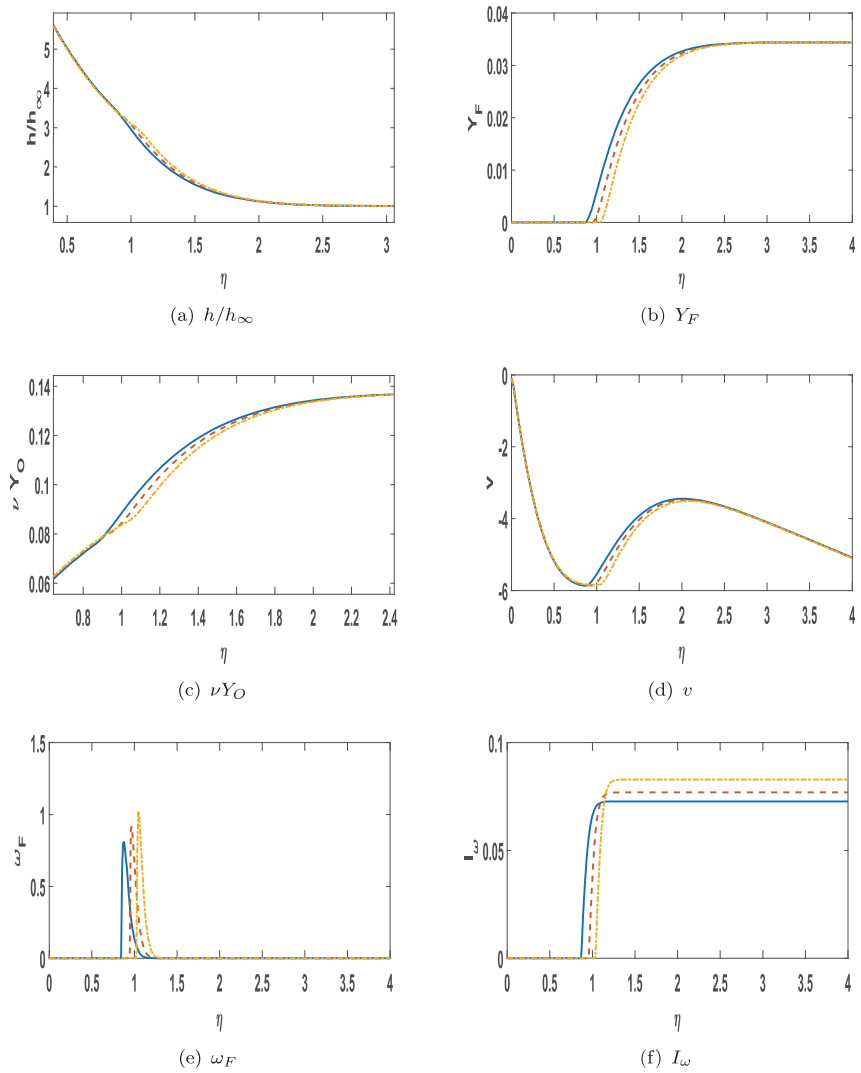

Figure 8. Lean premixed flame at various values of *Da*. $Y_{F,\infty} = 0.0344$, $Y_{O,\infty} = 0.500$, $K = 0.3$ blue solid, 1.0 red dashed, 3.0 orange dot-dash. (a) h/h_∞. (b) Y_F. (c) νY_O. (d) v. (e) ω_F. (f) I_ω.

see the burning rate increasing in proportion to the square root of the *Da*. Heat diffusion appears to be controlling here in both cases.

In general,sensitivity of the flame solution to *Da* is weaker than the sensitivity to the other studied parameters: mixture ratio, wall temperature, and *Pr*. This strengthens argument about diffusion control.

3.4. *Effect of Prandtl number*

An increase in *Pr* essentially is a decrease in the thermal conductivity and mass diffusivity values resulting in expected increased scalar gradients as shown in Figure 10 for the very

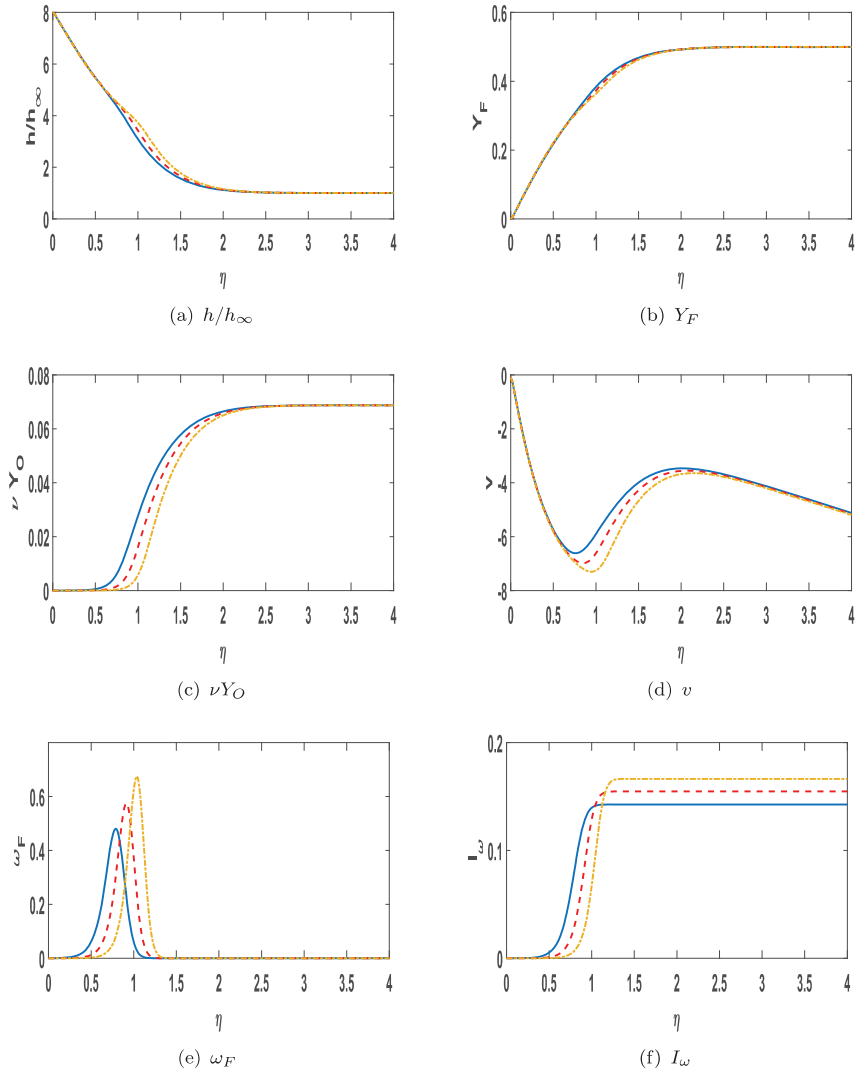

(a) h/h_∞ (b) Y_F

(c) νY_O (d) v

(e) ω_F (f) I_ω

Figure 9. Rich premixed flame at various values of Da. $Y_{F,\infty} = 0.500$, $Y_{O,\infty} = 0.250$, $K = 0.3$ blue solid, 1.0 red dashed, 3.0 orange dot-dash. (a) h/h_∞. (b) Y_F. (c) νY_O. (d) v. (e) ω_F. (f) I_ω.

lean mixture and in 11 for the very rich mixture. Thus, faster heat conduction occurs as Pr increases from 0.7 to 1.3. The global burning rate I_ω increases with the increased heat transfer rate from the wall to the flame, indication again diffusion control. Note that fuel and oxygen transport to the flame by both advection and diffusion. Advection at the flame front is reduced with increasing Pr, i.e. $|v|$ becomes smaller. Thus, the increase in mass diffusion rates must increase strongly to overcome that disadvantage and allow the increased burning rate.

Interesting comparisons can be made between Figures 8 and 9 on one side and Figures 10 and 11 on the other side. Notably, small changes in heat and mass diffusivities

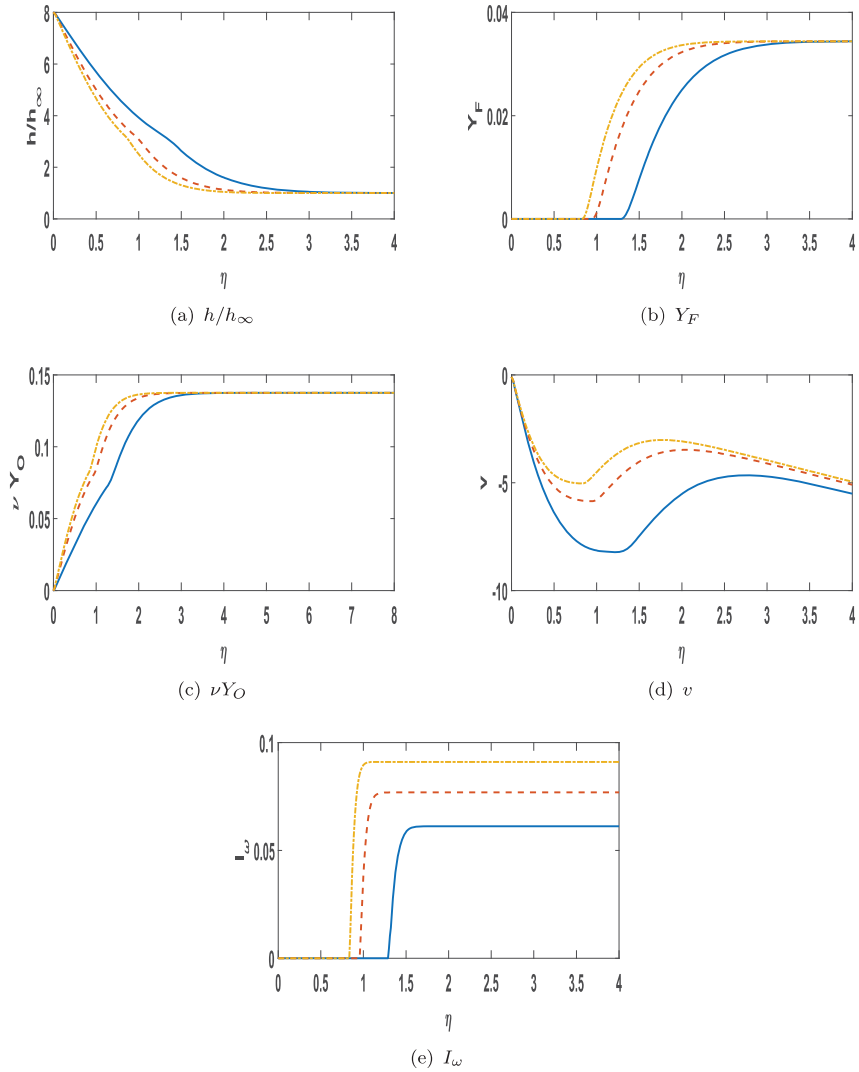

(a) h/h_∞ (b) Y_F

(c) νY_O (d) v

(e) I_ω

Figure 10. Lean premixed flame at various Prandtl numbers: scalar properties. $Y_{F,\infty} = 0.0344$, $Y_{O,\infty} = 0.500$, $Pr = 0.7$ blue solid, 1.0 red dashed, 1.3 orange dot-dash. (a) h/h_∞. (b) Y_F. (c) νY_O. (d) v. (e) I_ω.

have stronger effects on burning rates than an order-of-magnitude change in Damköhler number. This is another strong indicator of diffusion control of premixed flames in the multi-branched flame context.

4. Conclusions

The use of a hot wall in a stagnation-point flow is a reasonable surrogate for examining the influence of a diffusion flame on a premixed flame in a multi-branched flame configuration.

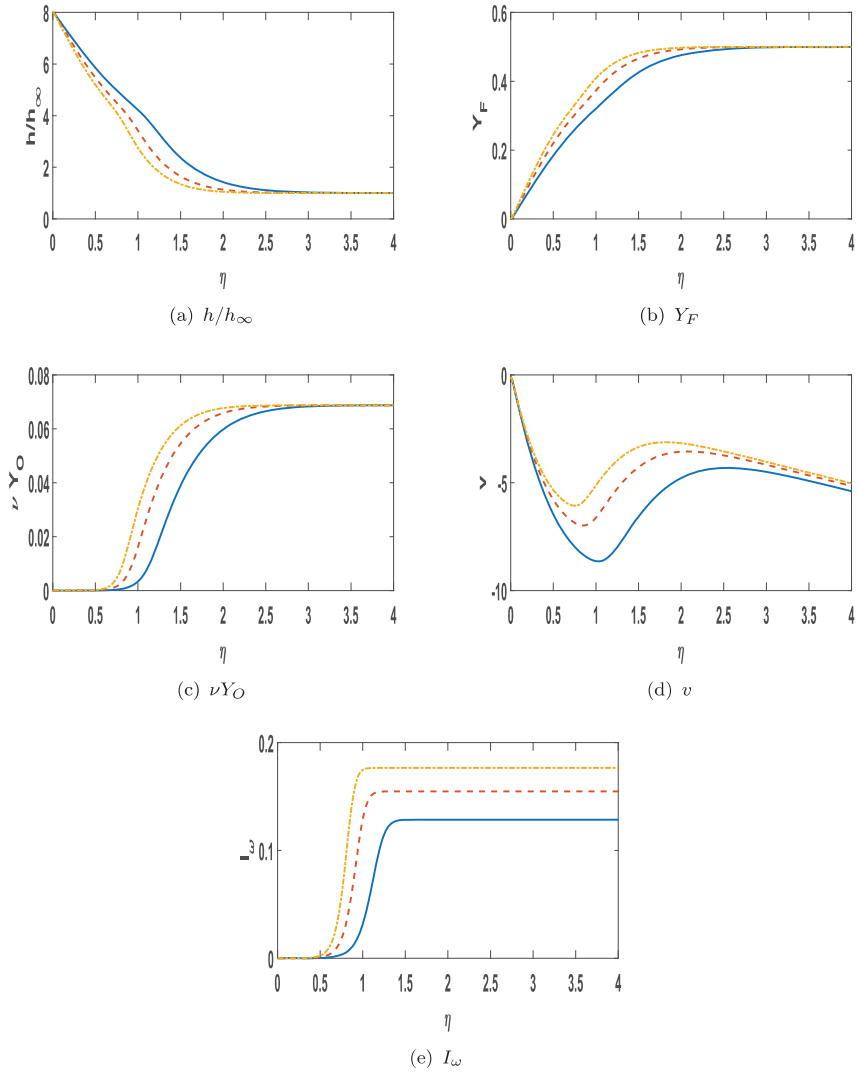

(a) h/h_∞ (b) Y_F (c) νY_O (d) v (e) I_ω

Figure 11. Rich premixed flame at various Prandtl numbers: scalar properties. $Y_{F,\infty} = 0.500$, $Y_{O,\infty} = 0.250$, $Pr = 0.7$ blue solid, 1.0 red dashed, 1.3 orange dot-dash. (a) h/h_∞. (b) Y_F. (c) νY_O. (d) v. (e) I_ω.

The configuration misses the effect of the diffusion of radical species from the diffusion flame to the premixed flame; however, in our one-step-kinetic model, the radicals are not resolved.

For mixture ratios sufficiently close to stoichiometric conditions for our propane-oxygen mixture, the flame stands outside of the wall diffusion layer and shows no reliance of heat transfer from the wall. For mixtures that are still more lean or still more rich, strong dependence on heat from the wall is shown for the premixed-flame sustenance. Those

flames stand in the wall diffusion layer and, as the wall temperature decreases, the flame weakens.

For these flames which stand in the wall diffusion layer, the dependence on *Da* is very slight. The dependence on *Pr* and therefore on transport properties is stronger. Thus, there is clear evidence of diffusion control with only slight kinetic influence. These findings are consistent with previous reporting of the penta-sectional nature of triple flame structures [19].

Acknowledgments

This research was supported by the Air Force Office of Scientific Research under Grant FA9550-18-1-0392 with Dr. Mitat Birkan as the scientific officer.

Disclosure statement

No potential conflict of interest was reported by the author(s).

Funding

This work was supported by Air Force Office of Scientific Research [grant number FA9550-18-1-0392].

References

[1] M. Matalon, *On flame stretch*, Combust. Sci. Technol. 31 (1983), pp. 169–181.
[2] M. Matalon and B.J. Matkowsky, *Flames as gasdynamic discontinuities*, J. Fluid. Mech. 124 (1982), pp. 239–259.
[3] J. Buckmaster and M. Matalon, *Anomoualous lewis number effects in tribrachial flames*, Proc. Twenty-Second Symp. (Int.) Combust. 22 (1988), pp. 1527–1535.
[4] A. Linan, *The asymptotic structure of counterflow diffusion flames for large activation energies*, Acta Astonautica 1 (1974), pp. 1007–39.
[5] F.E. Marble, *Growth of a diffusion flame in the field of a vortex*, in *Recent Advances in the Aerospace Sciences*, Plenum Press, New York, 1985, pp. 395–413.
[6] A.R. Karagozian and F.E. Marble, *Study of a diffusion flame in a stretched vortex*, Combust. Sci. Technol. 45 (1986), pp. 65–84.
[7] B.M. Cetegen and W.A. Sirignano, *Study of molecular mixing and a finite rate chemical reaction in a mixing layer*, in *Proceedings of Twenty-Second Symposium (International) on Combustion*, Combustion Institute, Pittsburgh, 1988, pp. 489–94.
[8] B.M. Cetegen and W.A. Sirignano, *Study of mixing and reaction in the field of a vortex*, Combust. Sci. Technol. 72 (1990), pp. 157–81.
[9] N. Peters, *Turbulent combustion*, 1st ed., Cambridge University Press, Cambridge, 2000.
[10] C. Pierce and P. Moin, *Progress-variable approach for large-eddy simulation of non-premixed turbulent combustion*, J. Fluid. Mech. 504 (2004), pp. 73–97.
[11] T. Nguyen, P. Popov, and W.A. Sirignano, *Longitudinal combustion instability in a rocket motor with a single coaxial injector*, J. Propul. Power 34(2) (2018), pp. 354–373.
[12] T. Nguyen and W.A. Sirignano, *The impacts of three flamelet burning regimes in nonlinear combustion dynamics, invited paper*, Combust. Flame 195 (2018), pp. 170–182.
[13] A. Hamins, H. Thridandam, and K. Seshadri, *Structure and extinction of a counterflow partially premixed, diffusion flame*, Chem. Eng. Sci. 40 (1985), pp. 2027–2038.
[14] W.A. Sirignano, *Counterflow and wall stagnation flow with three-dimensional strain*, Phys. Fluids 31 (2019), p. 053605. doi:10.1063/1.5096472.
[15] W.A. Sirignano, *Combustion with multiple flames under high strain rates*, Combust. Sci. Technol. 192 (2019). doi:10.1080/00102202.2019.1685507.

[16] C.F. López-Cámara, A. Jordà Juanós, and W.A. Sirignano, *Normal strain rate and pressure effects using detailed and global chemistry models in a* CH_4*-air counterflow flame*, Western States/ Combustion Institute Meeting, Albuquerque, 2019.
[17] C.F. López-Cámara, A. Jordà Juanós, and W.A. Sirignano, *Strain rate and pressure effects on multi-branched counterflow flames*, Combust. Flame 221 (2020), pp. 256–269.
[18] W.A. Sirignano, *Mixing and combustion in a laminar shear layer with imposed counterflow*, J. Fluid. Mech. 908 (2020).
[19] A. Jordà Juanós and W.A. Sirignano, *Triple flame: inherent asymmetries and pentasectional character*, Combust. Theory Model. 18 (2014), pp. 454–473.
[20] P. Rajamanickam, W. Coenen, A.L. Sanchez, and F.A. Williams, *Influences of stoichiometry on steadily propagating triple flames in counterflows*, Proc. Combust. Inst. 37 (2019), pp. 1971–1977.
[21] C.K. Westbrook and F.L. Dryer, *Chemical kinetic modeling of hydrocarbon combustion*, Prog. Energy Combust. Sci. 10 (1984), pp. 1–57.
[22] F. White, *Viscous Fluid Flow*. 3rd ed., McGraw-Hill, New York, 2006.